

## Crystal-field splitting in coadsorbate systems: $c(2\times 2)$ CO/K/Ni(100)

J. Hasselström, A. Föhlisch, R. Denecke,<sup>\*</sup> and A. Nilsson  
*Department of Physics, Uppsala University, Box 530, S-751 21 Uppsala, Sweden*

F. M. F. de Groot  
*Department of Inorganic Chemistry, Debye Institute, University of Utrecht, Sorbonnelaan 16, 3584 CA Utrecht, The Netherlands*  
(Received 7 June 1999; revised manuscript received 1 May 2000)

It is demonstrated how the crystal field splitting (CFS) fine structure can be used to characterize a coadsorbate system. We have applied K  $2p$  x-ray absorption spectroscopy (XAS) to the  $c(2\times 2)$  CO/K/Ni(100) system. The CFS fine structure is shown to be sensitive to the local atomic environment, the level of interaction, and the chemical state of the alkali atoms. From angle dependent XAS measurements, combined with x-ray photoelectron spectroscopy, a significant K-CO electrostatic adsorbate-adsorbate interaction is found, whereas the K-Ni interaction is substantially weaker. The present results provide evidence for a coadsorbed overlayer best described in terms of the properties associated with an ionic (two-dimensional) crystal.

### I. INTRODUCTION

In many metal complexes, the degeneracy of the  $d$  orbitals is lifted due to the symmetry reduction around the central ion potential. In the external field of neighboring atoms the metal  $d$  levels split into sublevels, an effect often referred to as crystal-field splitting (CFS).<sup>1,2</sup> The CFS fine structure is sensitive to both the local geometry of the system, and to the level of interaction of the metal atoms with, e.g., the ligands.<sup>3,4</sup> This has enabled the extraction of important chemical properties for a variety of different bulk compounds, surfaces, and interfaces, see, e.g., Refs. 4 and 5. In the present work we demonstrate how the CFS can be used in order to investigate coadsorbate systems. We have applied K  $2p$  x-ray absorption spectroscopy (XAS) to the  $c(2\times 2)$  CO/K/Ni(100) system, where the CFS fine structure is found to reveal detailed information about the interaction and chemical state of the alkali atoms. XAS is characterized by the excitation of a core electron to an unoccupied electronic level, or into the continuum.<sup>6</sup> In the soft x-ray regime, the process is governed by the dipole selection rule,<sup>7</sup> implying that the metal  $d$  levels can be reached through the K  $2p \rightarrow 3d$  transition.

Alkali adsorption on metal surfaces can, in many respects, be characterized by the behavior of the work function. It has been shown that for low coverage, the alkali atoms have the tendency to transfer their valence  $s$  electron to the substrate. When increasing the coverage, charge is partly withdrawn resulting in a saturated neutral K monolayer exhibiting metallic properties on most transition metals.<sup>8,9</sup> The CO-metal bond is strengthened by the presence of K, see, e.g., Refs. 10–12; based on single crystal microcalorimeter measurements,<sup>11</sup> and scanning tunneling microscopy,<sup>13</sup> it has been suggested that a considerable part of the increased adsorption heat stems from a reionization of the K layer, giving rise to a long range electrostatic contribution, as an ionic K-CO lattice is formed.<sup>13,14</sup> By combining XAS with x-ray photoelectron spectroscopy (XPS), we have, for the case of

the alkali atoms, been able to draw conclusions supporting this picture.

The presence of a surface (or an interface) breaks the three-dimensional crystal symmetry. This inherently induces anisotropic field effects, with a CFS fine structure exhibiting angular dependence.<sup>5</sup> The two-dimensional ionic character of the present system is expected to induce particularly large spectral differences. A series of XAS spectra were thus recorded with the electric field vector ranging from parallel to the surface to  $15^\circ$  off the surface normal. The results enable us to characterize the K-Ni interaction, as compared to, e.g., the adsorbate-adsorbate interaction. The symmetry reduction around the K ion potential additionally increases the possible number of XAS final states. In the present case ( $C_{4v}$  symmetry) the total number of final states is 22 (e.g., Ref. 15); for the  $c(2\times 2)$  CO/K/Ni(100) phase, both the K and the CO have been proposed to occupy fourfold hollow sites.<sup>13,16,17</sup> Thus, in order to properly assign the observed spectral features we have chosen to correlate the experimental spectra with atomic multiplet calculations. In the model used, the local environment in the solid is taken into account as the adaptation of the spherically symmetric atomic field.<sup>4</sup> By using the same crystal-field parameters that are found adequate for the comparison with experiment but neglecting multiplet effects, information about the ground state  $d$  electronic structure has additionally been extracted.

### II. TECHNICAL DETAILS

The experiments were carried out at Beamline 22, at MAX-lab, the Swedish synchrotron radiation facility. The beamline is equipped with a modified SX-700 plane grating monochromator and a hemispherical electron energy analyzer [Scienta SES-200 (Ref. 18)]. XAS spectra were recorded in Auger electron yield mode (the potassium  $LMM$  transitions), with an energy resolution of 0.2 eV; for the present coadsorbate system the Auger yield mode possesses a distinct advantage since it enables a separation between the C  $1s$  and K  $2p$  XAS edges. The spectra were normalized to

the photon throughput and corrected for substrate backgrounds. The XPS spectra were recorded with a photon energy of 400 eV and with an overall resolution of about 0.35 eV.

Potassium was evaporated from an outgassed SAES getter source. At a sample temperature of 100 K, multilayers were deposited, as judged by the K  $2p$  XPS core levels; the multilayer shows a distinct chemical shift towards higher binding energy, as demonstrated, e.g., on Pt(111) in Ref. 19. The alkali monolayer is prepared by flashing the crystal to 350 K. The  $c(2 \times 2)$  CO/K/Ni(100) phase was prepared by subsequent dosing of 20 L CO ( $1\text{L} \equiv 1 \times 10^{-6}$  torr s) at elevated temperatures (300–420 K). The preparations were monitored by a combination of low-energy electron diffraction (LEED) and XPS. All measurements were performed at 90 K.

Computationally, the atomic excitation from K  $2p^6 3d^0$  to K  $2p^5 3d^1$  was calculated for a  $K^+$  ion by means of a dipole transition, with the inclusion of the crystal field. This approach is based on the premise that the interaction of the core hole with the excited electron dominates over the interaction with neighboring atoms, and has proven useful for a large number of systems.<sup>4,5</sup> Solid state effects are included as additional crystal-field terms that are added to the Hamiltonian. These are treated as free parameters and were allowed to vary to obtain the best fit to experiment. In  $C_{4v}$ , the dipole operator is split, enabling polarization dependent spectra to be calculated. Two spectra were thus calculated, corresponding to  $\vec{E}$  normal and parallel to the surface, respectively; any given angle may be obtained with these spectra, using the well known relations for angular distribution of XAS resonances.<sup>6</sup> All theoretical spectra have been broadened by a Lorentzian with a full width at half maximum (FWHM) of 0.2 eV to simulate the lifetime broadening, and with a Gaussian (FWHM=0.4 eV).

### III. RESULTS AND DISCUSSION

In the upper panel of Fig. 1, the K  $2p \rightarrow 3d$  XAS spectra are shown for the clean alkali monolayer and the coadsorbed system. The spectra were recorded with the electric field vector parallel to the surface. This consequently means that the electronic states with an orbital amplitude parallel to the surface plane are probed. The K/Ni(100) spectrum contains essentially two components, situated at about 296.5 and 299.5 eV, respectively. These are the  $2p_{3/2}, 2p_{1/2} \rightarrow 3d$  transitions. The very broad spectral features are indicative for an alkali overlayer exhibiting metal character. Starting at about 293 eV a distribution of weak states are additionally found. Since the radial matrix element is about 10–100 times larger for  $d$  final states compared to  $s$  final states in K  $2p$  XAS,<sup>20</sup> the distribution seems dominated by K  $3d$  hybrids, but likely also carries some K  $4s$  signature.

The coadsorbed CO induces dramatic changes to the absorption spectrum. First, the spectral features get much narrower. This can be attributed to a loss of metallic character (reionization); the reduced metal-metal overlap induces a transformation from the unoccupied valence electron  $d$  band to, more or less, individual atomic  $d$  orbitals. Second, the  $d$  orbitals appear to be split into two lines, separated by about 1.2 eV. The appearance of these spectral features could

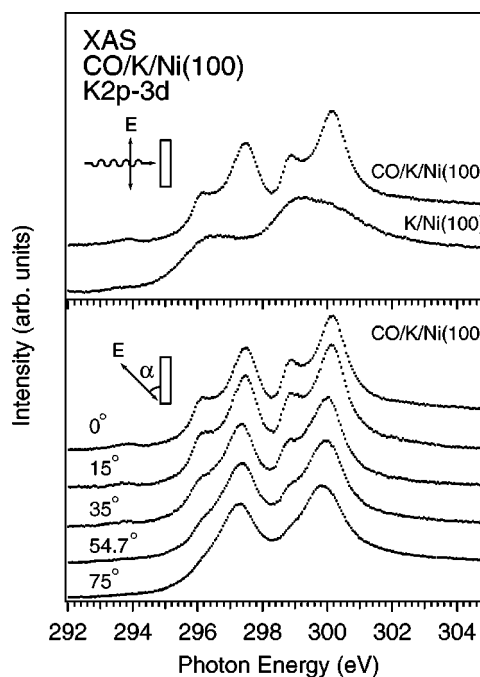


FIG. 1. Upper panel: K  $2p \rightarrow 3d$  XAS spectra obtained for K/Ni(100) and CO/K/Ni(100), with the  $E$  vector parallel to the surface. Lower panel: K  $2p \rightarrow 3d$  XAS spectra obtained for CO/K/Ni(100); the angle  $\alpha$  is given as the deviation of the electric field vector from the surface plane.

readily be assigned to an induced crystal field, where the observed  $d$  components may be viewed as having different relative orientation with respect to the field. We would, however, like to point out that the detailed effect of the crystal field is not that the atomic lines are split into two different components. Because of the strong interaction of the  $2p$  core and the  $3d$  valence wave functions, a large number of states are accessible. The present  $2p^5 3d^1$  final state gives rise to, e.g., three levels for an atom, seven levels with a cubic crystal field, and 22 individual components for the case of  $C_{4v}$  symmetry.<sup>21</sup> The crystal field has the effect of shifting these states in energy and redistributing the absorption intensity over all lines.

Additional information about the level of interaction of the alkali atoms with its neighbors can be obtained by angle resolved XAS measurements. In particular, this enables us to characterize the K-Ni interaction as compared to, e.g., the adsorbate-adsorbate interaction. The data are depicted in the lower panel of Fig. 1. A clear angular variation of the spectral shapes is observed. When the  $E$  vector approaches the surface normal the double peaked structure gradually disappears on the expense of an essentially single peaked spectral feature. This indicates substantial anisotropic field effects within the coadsorbate layer, i.e., as compared to along the surface normal. Additionally, the XAS cross section to the alkali  $d$  states is different for in-plane and out-of-plane polarization.<sup>6</sup> In the present work a coordinate system where the  $z$  direction is directed along the surface normal is adapted. The maximum amplitude of the  $d_{x^2-y^2}$  orbital is directed towards the CO molecules and the  $d_{xy}$  orbitals towards neighboring alkali atoms. For normal incidence the  $E$  vector lies in the plane and in principle all states are allowed by selection rules; the  $d_{z^2}$  state will, however, have very low

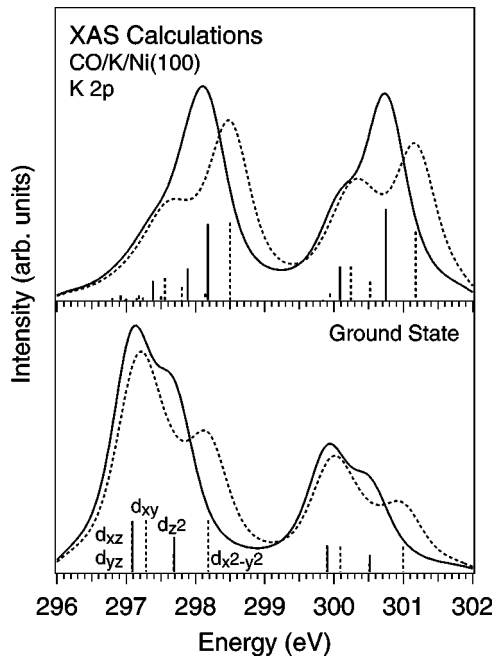


FIG. 2. Upper panel: Crystal field multiplet calculation of a  $K^+$  ion in  $C_{4v}$  symmetry. The  $Dq$ ,  $Ds$ , and  $Dt$  parameters (given in the text) have been optimized to experiment. Lower panel: Exactly the same calculation with the  $2p3d$  overlap (i.e., the multiplet effect) set to zero. The four symmetry states are directly visible. The  $0^\circ$  spectra are given with dashed lines and sticks and the  $75^\circ$  spectra with solid lines and sticks.

intensity. In the case of grazing incidence, the  $E$  vector points out of the  $xy$  plane and only the  $d_{xz}/d_{yz}$  and the  $d_{z^2}$  states can essentially be reached. The broad spectral shapes and the large number of allowed XAS final states make it difficult to assign the spectral features in detail without the explicit use of theory. The present calculations assume  $K^+$  ions giving rise to relatively simple multiplet calculations, where the ground state can be assumed to be  $2p^63d^01S_0$ .

The  $2p$  XAS process creates a  $2p^53d^1$  final state where the dominating effect on the spectral shape is the overlap of the  $2p$  and  $3d$  wave functions, the so-called multiplet effect.<sup>22</sup> The large core hole spin-orbit coupling makes it impossible to use a  $LS$  coupling scheme to describe the final states. The multiplet calculations are thus performed in the intermediate coupling case; if a large core hole spin orbit splitting is present no simple relation to the  $LS$  coupling scheme can be made. If we initially neglect the multiplet interaction, an XAS process where a single  $2p$  electron is put into the  $3d$  orbitals of the  $K^+$  ion is obtained. In  $C_{4v}$  symmetry, there are four different energy levels, related to the  $d_{x^2-y^2}$  orbital, the  $d_{z^2}$  orbital, the  $d_{xy}$  orbital, and the degenerate  $d_{xz}$  and  $d_{yz}$  orbitals, respectively. For this simple case, the angle integrated XAS spectra will, for both the  $L_3$  and the  $L_2$  edges consequently consist of four peaks with an intensity ratio that mimics the degeneracy of the four  $d$  states, i.e., 1:1:1:2 (cf. Fig. 2).

When accounting for multiplet effects, the single particle picture, in which one can relate the spectral features to orbitals in the ground state electronic structure, has to be modified. To illustrate this convincingly, the upper panel of Fig. 2 shows the theoretical simulation of the experiment, while the

lower panel shows the same calculation, but with the  $2p3d$  overlap set to zero. The orbital states in the calculated spectrum are completely mixed and their intensities are distributed over the 22 possible  $2p^53d^1$  final states. The procedure to determine the optimized fit was the following: In  $C_{4v}$ , there are three parameters that determine the positions of the  $3d$  orbitals,  $Dq$ ,  $Ds$ , and  $Dt$ , with the cubic crystal field splitting being  $10Dq$ .<sup>4</sup> The energies of the four  $d$  states are directly given by the three parameters as  $E(d_{x^2-y^2}) = 6Dq + 2Ds - Dt$ ,  $E(d_{z^2}) = 6Dq - 2Ds - 6Dt$ ,  $E(d_{xy}) = -4Dq + 2Ds - Dt$ , and  $E(d_{xz}/d_{yz}) = -4Dq - Ds + 4Dt$ .<sup>22</sup> The calculated spectrum of Fig. 2 simulates the experimental spectral distribution very well. Best overall agreement with the experimental spectra is obtained for the crystal field parameters,  $10Dq = 0.9$  eV,  $Ds = 0.1$  eV, and  $Dt = 0.02$  eV. The double peaked  $0^\circ$  spectrum and the essentially single peaked  $75^\circ$  spectrum are reproduced. The peak shift between the  $0^\circ$  and  $75^\circ$  spectra is exactly reproduced. A slightly larger energetic distance between the two main spectral features is found in the experiment (1.2 eV), as compared to the calculations (0.9 eV). This can be partly due to the  $10Dq$  value, but the relation between experimental peak distance and the value of  $10Dq$  is complex and the present choice of parameters does yield the most satisfactory agreement on all aspects of the experimental shape. Note that the intensity ratio of the two peaks in both the  $L_2$  and the  $L_3$  edge are calculated correctly. The good agreement with experiment, in particular the correctly simulated angular variations, make us confident about the values of the crystal field parameters.

In the lower panel of Fig. 2, the atomic  $2p3d$  overlap (the multiplet effect) has been turned off. This yields the single particle spectral shape related to the same crystal-field parameters as in the case of the multiplet spectrum. One of the advantages of the single particle spectrum is that one can immediately pinpoint the four  $d$  states. To a first approximation we thus project out the ground state K valence  $d$  states (in the presence of a noninteracting K  $2p$  core hole). The electronic states at the lowest energy are the  $d_{xz}/d_{yz}$  orbitals; the  $d_{xz}$  orbital is situated at 0.2 eV higher energy. Additionally, the  $d_{z^2}$  orbital has a relative energy of 0.6 eV and the energetically highest state is the  $d_{x^2-y^2}$  orbital at 1.1 eV. The relative energies of the four states enable us to draw conclusions about the bonding character of the K ions and its neighbors. The relative energy of the  $d$  states reflects the level of interaction, electrostatically as well as covalently, with the neighboring atoms. Independent on the exact symmetry, the high energy peaks are always related to states with a large interaction with its neighbors<sup>23</sup>. The fourfold variation of the charge density of the CO molecules essentially creates the 0.9 eV energy difference between the high-energy  $d_{x^2-y^2}$  orbital and the energetically lower  $d_{xy}$  orbital; the maximum amplitude of the  $d_{x^2-y^2}$  orbital is directed towards the CO molecules and the  $d_{xy}$  orbitals towards neighboring alkali atoms. The interaction between the  $d_{z^2}$  orbital and the Ni surface puts the  $d_{z^2}$  orbital 0.4 eV higher in energy as compared to the  $d_{xy}$  orbital. These results seem to indicate a relatively strong K-CO interaction and a substantially weaker K-Ni interaction. The  $d_{xy}$  orbitals are only weakly affected from the near-lying adsorbates and are found 0.2 eV above the (degenerate) lowest energy  $d_{xz}$  and  $d_{yz}$  states, which interact very strongly with neither the CO molecules nor the Ni surface.

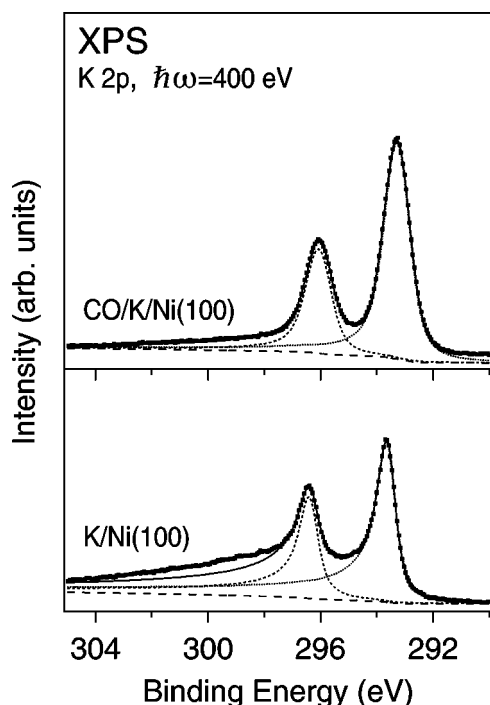


FIG. 3. K  $2p$  XP spectra obtained for K/Ni(100) and CO/K/Ni(100). The spectra were recorded using a photon energy of 400 eV. Included is also the result of a line shape analysis using a Doniach-Sunjic line profile (dotted lines).

The crystal-field splitting is caused by both ionic and covalent effects. In the computational model a total (ionic plus covalent) crystal field is used. Consequently, from the CFS values it is not possible to draw any conclusions regarding the ionic or covalent interaction within the coadsorbate overlayer. However, the XPS core level line shape is highly dependent on whether a system is metallic or ionic (insulator). In metallic systems, the XPS core level line shape has a characteristic asymmetry due to the multielectron response upon core-hole creation. This line shape has successfully been parametrized with the so-called Doniach-Sunjic line profile,<sup>24,25</sup> where an increasing level of metallic character is related to an increasing asymmetry, given by the asymmetry parameter  $\alpha$ . Our previous work has shown that the Doniach-Sunjic line profile is also fully applicable for adsorbed molecules,<sup>26,27</sup> which allows us to address, through the XPS line shapes and different asymmetries, the metallic character of the K monolayer and thus the issue whether parts of the alkali-induced increased CO adsorption energy can be related to a direct charge transfer interaction with the alkali adatoms, see, e.g., Ref. 12 and references therein.

In the lower panel of Fig. 3, the K  $2p$  XP spectrum is presented for a monolayer of K on Ni(100). Characteristic for the spectrum are the two spin-orbit components; the K  $2p_{3/2}$  binding energy is 293.8 eV while the K  $2p_{1/2}$  component is found at 296.5 eV. A detailed Doniach-Sunjic line profile analysis (dotted line in Fig. 3) using a Shirley background<sup>28</sup> gives for the K  $2p$  spin-orbit components (FWHM=0.8 eV) an asymmetry parameter of  $\alpha=0.19$ , which is a typical asymmetry value for the alkali metals.<sup>25</sup> In addition, by means of electron energy loss spectroscopy (EELS) a surface plasmon at about 2.7 eV, characteristic for metallic K has been observed.<sup>29–32</sup> This leads to additional

intensity not accounted for in the simple Doniach-Sunjic line profile. However, from a comparison to an XPS study conducted by Heskett *et al.* on K/Al(100),<sup>33</sup> we conclude that the surface plasmon cannot be clearly resolved (i.e., with K  $2p$  XPS) for the present system. The presence of CO induces significant changes to the alkali layer; the K  $2p$  XP spectrum for  $c(2\times 2)$  CO/K/Ni(100) is depicted in the upper panel of Fig. 3. Here the K  $2p_{3/2}$  binding energy is 293.3 eV while the K  $2p_{1/2}$  component is found at 296.0 eV. The most striking difference as compared to the K monolayer is the symmetric line shapes of the two main spectral features. The intensity from the electron shake up transitions is suppressed. This shows that upon CO adsorption, the K overlayer loses its metal character. This observation is additionally supported by the obtained asymmetry parameter in the line shape analysis, which was found to be  $\alpha=0.05$  (FWHM=1.0 eV).

Due to the large difference in electronegativity between K and CO, an essentially ionic CO/K overlayer would explain the above-mentioned observations, where the adsorbate-adsorbate interaction to a large extent is governed by electrostatics. This is additionally strengthened by the similarity of the present XAS spectra to those of the ionic alkali halides, e.g., KCl.<sup>3</sup> Upon coadsorption of CO, the K adatoms become screened from each other, inducing the observed metal-to-(near) insulator transformation. Similar conclusions have been drawn about the character of Cs in the CO/Cs/Co(0001) coadsorption system utilizing EELS.<sup>34,35</sup> Thus in the case of the periodic  $c(2\times 2)$  CO/K/Ni(100) there will be a long range electrostatic contribution to the adsorption heat, as an ionic K-CO lattice, and the corresponding mirror image charges in the substrate, is formed. It is, however, interesting to note that the XAS spectra (Fig. 1) does seem to indicate a certain level of charge transfer interaction. In the XAS spectra recorded with the  $E$  vector parallel to the surface plane there is a spectral feature present with a maximum intensity at about 293.8 eV. For the case of K/Ni(100), a weak distribution of states is observed in this spectral region, while the feature seems more localized for the coadsorbed system. Since the Fermi level is situated at 293.3 eV for the coadsorbate system, i.e., where the above-mentioned spectral feature starts to grow, a small, but non-negligible covalency between the alkali atoms, and possibly also between the CO and K adatoms cannot be ruled out. Both these interactions lower the effective charge on the potassium ions. The covalency can most likely be correlated to the very dense character of the  $c(2\times 2)$  CO/K/Ni(100) coadsorbate overlayer; for systems with lower initial alkali and CO coverages, essentially  $K^+$  ions are expected. We would, however, like to stress that based on, e.g., C  $1s$  and O  $1s$   $K$ -edge XAS and x-ray emission spectroscopy measurements on the present system, no new alkali related spectral features were observed.<sup>17</sup> We are thus confident that the ionic character of the K atoms dominates the adsorbate-adsorbate interaction; the crystal-field splitting is simply set by the ionic interaction within the ordered overlayer lattice.

#### IV. CONCLUSIONS

In conclusion, we have shown with XAS how the CFS fine structure may be used in order to characterize a coadsorption system. The CFS shows pronounced angular variations; these may readily be interpreted as due to strong interaction within the overlayer and a substantially weaker K-Ni

interaction. Our results provide experimental evidence for a two-dimensional ionic overlayer formation, with only a limited covalent interaction between the coadsorbate species. The local character of the XAS process implies that the results may be correlated using atomic multiplet theory, with the inclusion of the crystal field.

## ACKNOWLEDGMENTS

We would like to thank the staff at MAX-lab for all their assistance. This work was supported by Swedish Natural Science Research Council (NFR) and by Göran Gustafsson Foundation for Research in Natural Science and Medicine.

\*Present address: Universität Erlangen-Nürnberg, Lehrstuhl für Physikalische Chemie II, Egerlandstr. 3, D-91058 Erlangen, Germany.

- <sup>1</sup>C.J. Ballhausen, *Introduction to Ligand Field Theory* (McGraw-Hill, New York, 1962).
- <sup>2</sup>S. Sugano, Y. Tanabe, and H. Kamimura, *Multiplets of Transition Metal Ions in Crystals* (Academic, New York, 1970).
- <sup>3</sup>F. Sette, B. Sinkovic, Y.J. Ma, and C.T. Chen, *Phys. Rev. B* **39**, 11 125 (1989).
- <sup>4</sup>F.M.F. de Groot, *J. Electron Spectrosc. Relat. Phenom.* **67**, 529 (1994).
- <sup>5</sup>F.J. Himpsel, U.O. Karlsson, A.B. McLean, L.J. Terminello, F.M.F. de Groot, M. Abbate, J.C. Fuggle, J.A. Yarmoff, B.T. Thole, and G.A. Sawatzky, *Phys. Rev. B* **43**, 6899 (1991).
- <sup>6</sup>J. Stöhr, *NEXAFS Spectroscopy* (Springer-Verlag, Heidelberg, 1992).
- <sup>7</sup>R. Manne, *J. Chem. Phys.* **52**, 5733 (1970).
- <sup>8</sup>H.P. Bonzel, *Prog. Surf. Sci.* **42**, 219 (1993).
- <sup>9</sup>J.J. Weimer, E. Umbach, and D. Menzel, *Surf. Sci.* **159**, 83 (1985).
- <sup>10</sup>H.S. Luftman, Y.-M. Sun, and J.M. White, *Appl. Surf. Sci.* **19**, 59 (1984).
- <sup>11</sup>N. Al-Sarraf, J.T. Stuckless, and D.A. King, *Nature (London)* **360**, 243 (1992).
- <sup>12</sup>A. Görling, L. Ackermann, J. Lauber, P. Knappe, and N. Rösch, *Surf. Sci.* **286**, 26 (1993).
- <sup>13</sup>S.J. Murray, P. Finetti, F.M. Leibsle, R.D. Diehl, and R. McGrath, *Chem. Phys. Lett.* **237**, 474 (1995).
- <sup>14</sup>S.J. Murray and R. McGarth, *Surf. Sci.* **307-309**, 668 (1994).
- <sup>15</sup>S.-I. Nakai, H. Nakamori, A. Tomita, K. Tsutsumi, H. Nakamura, and C. Sugiura, *Phys. Rev. B* **4**, 1870 (1974).
- <sup>16</sup>O.B. Christensen and J.K. Nørskov, *Chem. Phys. Lett.* **214**, 443 (1993).
- <sup>17</sup>J. Hasselström, A. Föhlisch, P. Väterlein, A. Nilsson, M. Nyberg, and L. G. M. Pettersson (unpublished).
- <sup>18</sup>N. Mårtensson, P. Baltzer, P. Brühwiler, J.O. Forsell, A. Nilsson, A. Stenborg, and B. Wannberg, *J. Electron Spectrosc. Relat. Phenom.* **70**, 117 (1994).
- <sup>19</sup>G. Pirug, A. Winkler, and H.P. Bonzel, *Surf. Sci.* **163**, 153 (1985).
- <sup>20</sup>M.W.D. Mansfield, *Proc. R. Soc. London, Ser. A* **348**, 143 (1976).
- <sup>21</sup>Since the CFS is essentially the nonspherical effect of the chemical bonding, the influence from the CFS on the K  $2p$  levels can be neglected. The chemical bonding only affects the valence electrons. Thus the localized K  $2p$  core orbitals remain unaffected by nonspherical bonding effects.
- <sup>22</sup>P.H. Butler, *Point Group Symmetry, Applications, Methods and Tables* (Plenum, New York, 1981).
- <sup>23</sup>F.M.F. de Groot, J.C. Fuggle, B.T. Thole, and G.A. Sawatzky, *Phys. Rev. B* **41**, 928 (1990).
- <sup>24</sup>S. Doniach and M. Sunjic, *J. Phys. C* **3**, 285 (1970).
- <sup>25</sup>S. Hüfner, *Photoelectron Spectroscopy* (Springer-Verlag, Heidelberg, 1995).
- <sup>26</sup>A. Föhlisch, N. Wassdahl, J. Hasselström, O. Karis, D. Menzel, N. Mårtensson, and A. Nilsson, *Phys. Rev. Lett.* **81**, 1730 (1998).
- <sup>27</sup>A. Föhlisch, J. Hasselström, O. Karis, D. Menzel, N. Mårtensson, and A. Nilsson, *J. Electron Spectrosc. Relat. Phenom.* **101-103**, 303 (1999).
- <sup>28</sup>D.A. Shirley, *Phys. Rev. B* **5**, 4709 (1972).
- <sup>29</sup>J. Swan, *Phys. Rev. A* **135**, A1467 (1964).
- <sup>30</sup>S. Andersson and U. Jostell, *Surf. Sci.* **46**, 626 (1974).
- <sup>31</sup>S. Andersson and U. Jostell, *Solid State Commun.* **13**, 829 (1973).
- <sup>32</sup>S. Andersson and U. Jostell, *Solid State Commun.* **13**, 833 (1973).
- <sup>33</sup>D. Heskett, E. Lundgren, R. Nyholm, and J.N. Andersen, *Phys. Rev. B* **52**, 12 366 (1995).
- <sup>34</sup>P. He, Y. Xu, and K. Jacobi, *J. Chem. Phys.* **104**, 8118 (1996).
- <sup>35</sup>K. Jacobi, H. Shi, H. Dietrich, and G. Ertl, *Surf. Sci.* **331-333**, 69 (1995).